Study of a transferring system for measurements in aircraft assembly

Shuanggao Li, Zhichao Huang, Qi Zeng and Xiang Huang
College of Mechanical and Electrical Engineering, Nanjing University of Aeronautics and Astronautics, Nanjing, China

Received 9 January 2022
Revised 20 February 2022
Accepted 20 February 2022

Abstract

Purpose – Aircraft assembly is the crucial part of aircraft manufacturing, and to meet the high-precision and high-efficiency requirements, cooperative measurement consisting of multiple measurement instruments and automatic assisted devices is being adopted. To achieve the complete data of all assembly features, measurement devices need to be placed at different positions, and the flexible and efficient transfer relies on Automated Guided Vehicles (AGVs) and robots in the large-size space and close range. This paper aims to improve the automatic station transfer in accuracy and flexibility.

Design/methodology/approach – A transferring system with Light Detection and Ranging (LiDAR) and markers is established. The map coupling for navigation is optimized. Markers are distributed according to the accumulated uncertainties. The path planning method applied to the collaborative measurement is proposed for better accuracy. The motion planning method is optimized for better positioning accuracy.

Findings – A transferring system is constructed and the system is verified in the laboratory. Experimental results show that the proposed system effectively improves positioning accuracy and efficiency, which improves the station transfer for the cooperative measurement.

Originality/value – A Transferring system for collaborative measurement is proposed. The optimized navigation method extends the application of visual markers. With this system, AGV is capable of the cooperative measurement of large aircraft structural parts.

Keywords Transferring system, Visual marker, Laser tracker, Measurement

Paper type Research paper

1. Introduction

Aircraft assembly is one crucial part of aircraft manufacturing (Mei and Maropoulos, 2014), and to meet the high-precision and high-efficiency requirements, cooperative measurement consisting of multiple measurement instruments and automatic assisted devices is being adopted (Flynn and Miller, 2019). The data measured at a single position is limited and to achieve more data of all assembly features, measurement instruments need to be placed at different positions (Deng *et al.*, 2018). The flexible and efficient transfer relies on Automated Guided Vehicles (AGVs) and robots in the large-size space and close range, respectively. Manual handling of measuring instruments is inefficient for station transfer and unreliable in terms of accuracy, which will eventually reduce the measurement efficiency and accuracy (Deng *et al.*, 2018). With automatic station transfer, the efficiency of alignment can be improved as well (Zeng *et al.*, 2020a; Liu *et al.*, 2017; Mei and Maropoulos, 2014). Hence, it is of great significance to research on the automatic station transfer for the cooperative measurement in the field of aircraft manufacturing.

This research was supported by the Defense Industrial Technology Development Program (No. JCKY2018205A001). The authors declare no conflicts of interest.

Journal of Intelligent Manufacturing and Special Equipment
Vol. 3 No. 1, 2022
pp. 31-47
Emerald Publishing Limited
e-ISSN: 2633-660X
p-ISSN: 2633-6596
DOI 10.1108/JIMSE-01-2022-0001

Many navigation methods applied for automatic station transfer have been developed in recent years, which could be divided into three main categories according to the ranging devices (Ryck *et al.*, 2020; Andrea, 2012; Andreasson, 2015): (1) LiDAR (Light Detection and Ranging)-sensor-based type; (2) vision-sensor-based type; and (3) hybrid-sensors-based type. In those LiDAR-sensor-based methods, the navigation map is usually constructed with Simultaneous Localization and Mapping (SLAM), and it is superior in the performance of flexible navigation and active obstacle avoidance (Hess *et al.*, 2016; Ramasamy *et al.*, 2016). However, the transfer only relying on LiDAR is not accurate enough for cooperative measurement since positioning accuracy requirement in the efficient pre-alignment is almost 5 mm (Wu and Du, 2018). Speaking of the vision-based measurement, there are two main kinds: one kind is to build a map with the help of Visual Simultaneous Localization and Mapping (VSLAM) (Mur-Artal *et al.*, 2015; Mur-Artal and Tardos, 2017), and the other kind is to recognize the visual markers. VSLAM has an advantage of map construction and perception of large-scale spaces while the visual markers based methods are more accurate in positioning. QR (Quick Response) code, AR Tag, ArUco Marker (Garrido-Jurado, 2014), April Tag (Olson, 2011; Wang and Olson, 2016) and so on are the most common visual markers, and among them, April Tag (Xing *et al.*, 2018) is outstanding for easier identification and higher positioning accuracy (Krogius *et al.*, 2019). With markers as reference, the positioning is more convenient, and less or no interference of ambient light will happen. In view of this, this way is more applicable for transfer in the field of aircraft manufacturing. Wang *et al.* proposed a mobile robotic measurement system for large-scale complex components based on the visual markers (Wang *et al.*, 2021). But as Fiala *et al.* pointed out, the high positioning accuracy is limited to the periphery of markers, and for flexible transfer in the entire map, markers need to be combined with other methods (Fiala, 2015). Consequently, the hybrid method is developed to fuse information from different sensing devices, especially the hybrid of LiDAR and markers.

In the research of hybrid methods, Subramanian *et al.* effectively optimized the obstacle avoidance of Unmanned Aerial Vehicle UAV by the hybrid of LiDAR and visual navigation methods (Ramasamy *et al.*, 2016). Gao *et al.* improved the accuracy and flexibility, and the core is the occupancy map with markers integrated into it (Gao *et al.*, 2016). In recent studies, there are basically two main difficulties in this hybrid positioning system. The coupling accuracy is the prior factor for positioning accuracy, it is restricted by the ranging limitation of LiDAR. Besides, the position can be accurately achieved by measuring the close and fixed markers, and once the AGV moves away from the marker, the positioning accuracy decreases rapidly. So does the flexibility.

In terms of the coupling, it is optimized by the Adaptive Monte Carlo Localization (AMCL) in usual (Röwekämper *et al.*, 2012). For further optimization, Kudriashov *et al.* incorporated the EKF (extended Kalman filter) filtering into AMCL (Kudriashov *et al.*, 2019). The scene for the cooperative measurement is rarely changed and the measurement of AGV's positions for AMCL can be more accurate. The laser tracker is the high-precision measurement instruments and is indispensable in the cooperative measurement, which can be adapted for the measurement of AGV. The coupling can be improved by the more accurate positions of AGV. Based on this, the method of map construction is proposed and the conversion matrix of the coupling can be calculated. For the deficiency in flexibility, Zeng *et al.* fixed QR codes in the circular route and then the positions can be calibrated periodically (Zeng *et al.*, 2019). Wang *et al.* arranged markers in a certain density to calibrate the positioning (Wang *et al.*, 2021). The transfer in the measurement area demands high positioning accuracy, and quantitative analysis of various possible deviations is the premise of marker's layout. In view of this, the proposed method quantifies the deviations, assumes and verifies the relationship between the interval of markers and the various accumulative deviations. Based on this relationship, the layout of markers is reasonably estimated and applied.

In addition, the navigation method is changed adaptively as well. The entire navigation is segmented into several segments to recognize the markers, and in case of the damage of measurement instruments, the cost of path planning takes the changes of direction into consideration. Then the A^*-heuristic algorithm (A^*) is adapted accordingly. The measurement accuracy of the odometry decreases with distance, and due to the calibration of markers, the distance away from makers in the proposed map is very short. Hence, odometry and markers are adapted for the adjustment as accurate references. Together with the prearrangement and navigation method, the navigation system via LiDAR and markers is constructed for cooperative measurement in the field of aircraft manufacturing.

The rest of the paper proceeds in the following order. Section 2 briefly describes the structure of the system. Section 3 shows the method of map coupling and layout of markers. Section 4 explains the optimization of navigation methods in detail. The experiments of the self-positioning and navigation methods are evaluated and discussed in Section 5. Then, the conclusions and the future work are shown in Section 6.

2. System structure

The transferring system can be applied to the wing and fuselage assembly as shown in Plate 1. The proposed navigation system consists of the following equipment (Qin *et al.*, 2016):

(1) AGV with mecanum-wheels for flexible and accurate station transfer;

(2) LiDAR on board for map construction and obstacle avoidance;

(3) A camera on board for marker recognition and position calibration;

(4) Markers fixed on the ground for position calibration and map construction, which are also the core of path planning;

(5) A laser tracker for the assistance of map construction and verification of the accuracy in positioning.

The actual scene is scanned by LiDAR and the occupancy grid map is constructed with SLAM. The coordinates of markers and AGV are measured to optimize the coupling by the laser tracker with higher positioning accuracy. When the conversion matrix of two maps is decoupled, markers can be coupled into the grid map accordingly. For better path planning, segmented navigation method is adapted for periodic calibration with markers. A^* is optimized to select the path with the least cost and minimize the changes in direction to improve the reliability during the station transfer. Boundary marker is the marker closest to the target station, which is chosen to improve the final positioning accuracy. The procedure of the proposed navigation system can be simplified as Figure 1.

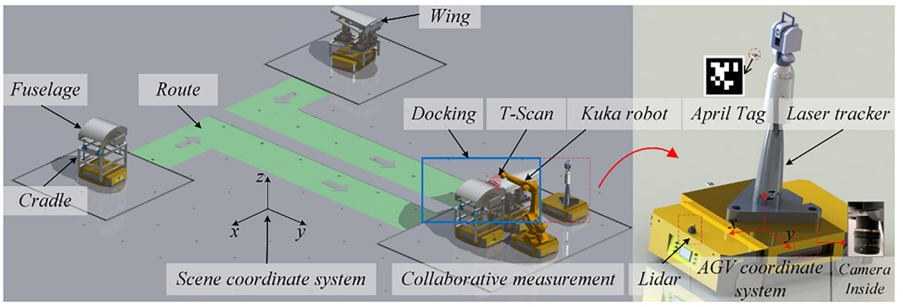

Plate 1.
An application of wing and fuselage assembly. Fuselage, wing and other measurement instruments are transferred by AGV, and two coordinate systems are constructed for navigation

3. Map construction

During the map coupling, the relative positions of AGVs are usually estimated by the odometry, which can be optimized by the laser tracker. And there is a problem that the target ball cannot locate the center of AGV.

Aiming at the problem, a fitting circle measurement method is proposed. The geometric center of Spherically Mounted Retroreflectors (SMRs) does not coincide with the center of AGV, but the relative positions of SMRs are fixed. When AGV rotates, the geometric center of SMRs is distributed in a circle around the geometric center of AGV as shown in Figure 2. AGVs rotate multiple times to calibrate the deviation between the center of SMRs and the center of AGV, where p_{Rj}^{k} denotes the center of SMRs and N_R denotes the times of rotation.

The center point set is obtained through rotation, and it can be fitted to a circle with P_{mid} as the center and r_{mid} as the radius. Therefore, the Total Least-Squares (TLS) equation (Coope, 1993), the geometric center of SMRs can be constructed. The problem of determining the circle of best fit, in a TLS scene, to a set of data points $P_{Rj} \in R^n$, $j = 1, 2, \ldots, N_R$, is a special case ($n = 2$) of the following TLS problem: Determining values of P_{mid} and r_{mid} which solve the problem:

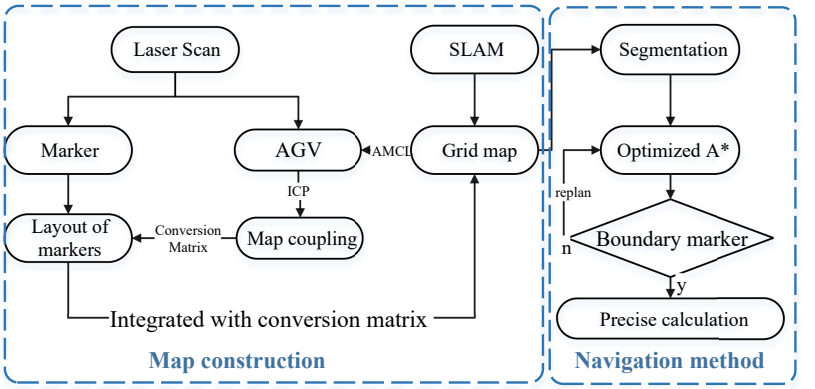

Figure 1.
The proposed navigation system consists of map construction and navigation method and map construction is the prearrangement for navigation method

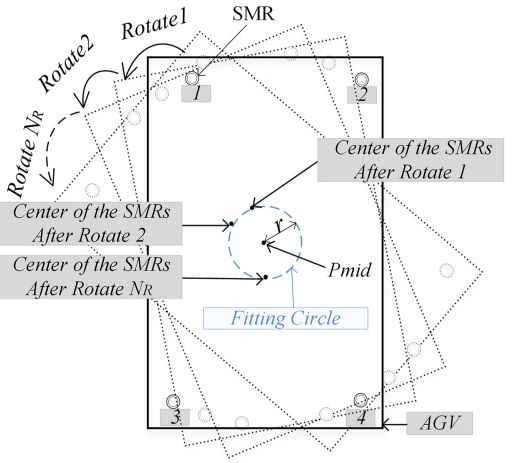

Figure 2.
The fitting circle measurement method is proposed for figuring out the geometric center of AGV

$$\min_{P_{\text{mid}},r}\sum_{j=1}^{N_R}\{f_j(P_{\text{mid}},\, r_{\text{mid}})\}^2 \tag{1}$$

where $f_j(P_{\text{mid}},\, r_{\text{mid}})$ is the distance of the point P_{Rj} from the fitted circle,

$$f_j(P_{\text{mid}},\, r_{\text{mid}}) = r_{\text{mid}} - \|P_{\text{mid}} - P_{Rj}\|_2 \tag{2}$$

As shown in Plate 2, a right-hand Cartesian coordinate system is established. During the coupling, N_p scattered stations are arranged for measurement. p_i equals to P_{mid} at each station. $X = \{x_1, x_2, \ldots, x_{N_p}\}$ denotes the positions of AGV in the occupancy grid map (Vasiljevic *et al.*, 2016).

The Iterative Closest Point (ICP) algorithm matching method is used to minimize the coupling error function $E(R, t)$ of the two coordinate systems (Arun, 1987). Decoupling the two coordinate systems of actual scene and grid map and the rotation matrix R and translation vector t can be calculated.

Markers measured by the laser tracker are, $M = \{m_0, m_1, \ldots, m_{N_{bq}}\}$, where N_{bq} denotes the number of markers. A denotes the coordinates of markers in the occupancy grid map and it can be obtained by solving the following equation:

$$A = R \cdot M + t \tag{3}$$

Uncertainties are closely related to positioning accuracy and they are distributed in the following parts: measurement uncertainty from laser tracker σ_{LTS} (Zeng *et al.*, 2020b), coupling uncertainty σ_T, motion uncertainty σ_m, uncertainty of marker recognition σ_c and the positioning error of AGV σ (Motai and Kosaka, 2008). The functional relationship between uncertainties and positioning accuracy are calculated and verified by the simulation. σ_T denotes the coupling uncertainty, and it can be calculated according to equation (3).

To figure out the functional relationship, uncertainties are measured and recorded in different distances respectively. The data are fitted with different functions and the function image is shown in Figure 3. The safety margin coefficient C is designed to leave a margin for uncertainty analysis. The safety margin coefficient should be 1 when the uncertainties are absolutely correct. For the reliability of the equation, the measurement data are calculated under different coefficients and a completely linear distribution. And when $C = 1$, the calculated result is closer to the actual distribution. In this case, C is slightly greater than 1.

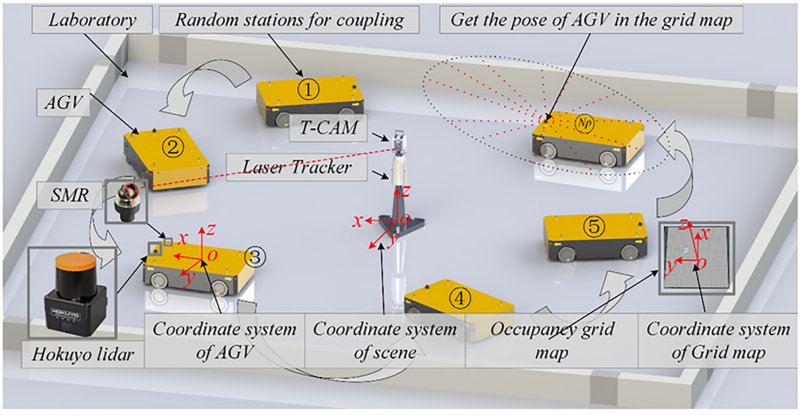

Plate 2.
The positions of AGV in the coordinate system of scene are measured in sequence by the laser tracker. The positions of AGV in the coordinate system of grid map are measured by LiDAR accordingly

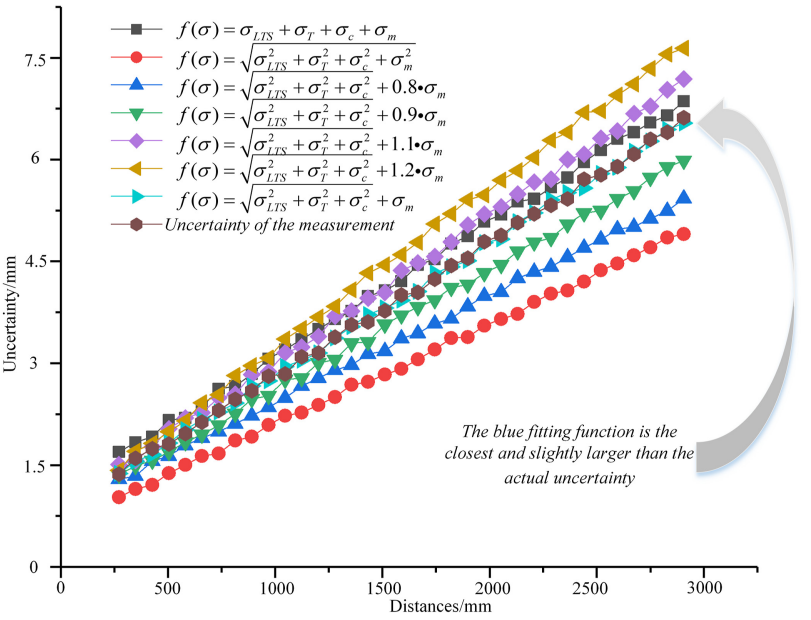

Figure 3.
Functional relationships between uncertainties and movement distances are simulated and the results of simulation are distinguished by different colors

$$\sigma = \sqrt{\sigma_{LTS}^2 + \sigma_T^2 + \sigma_c^2} + C\sigma_m \tag{4}$$

According to equation (5), the arrangement interval of markers d can be derived. The applicable interval should ensure that AGV can accurately identify the next adjacent marker after identifying one marker at least.

$$d = 2\frac{\left(\sigma - \sqrt{\sigma_{\mathrm{LTS}}^2 + \sigma_T^2 + \sigma_c^2}\right)}{C\sqrt{\sigma_x^2 + \sigma_y^2}} + d_{\mathrm{Tag}} - d_{\mathrm{FOV}} \tag{5}$$

where d_{Tag} denotes the size of markers and d_{Fov} denotes the square field of view.

Each interval needs to be less than d, but not to be strictly the same. Therefore, markers can be arranged and coupled into both actual scene and grid map, and the map for transferring is constructed.

Markers are easily contaminated and damaged and the arrangement of markers is time-consuming and troublesome, which are the limitations of the proposed marker based positioning method in actual measurement. Therefore, markers need to be checked and replaced regularly. Besides, the number of arranged markers can be reduced by planning the measurement area and other area in advance. As shown in Figure 4, 36 markers rather than 56 markers need deploying after the pre-planning.

4. Navigation method

Since the prearrangement of the system is completed, the navigation method is optimized accordingly. The navigation from the initial station to the boundary marker and from the

boundary marker to the target station is segmented as rough navigation and precise navigation respectively (see Figure 5).

The rough navigation is segmented into several segments and each segment is able to identify markers for position calibration, the difficulty of which is the accumulated errors.

Few markers are better for the efficiency, and the selection method can be obtained.

$$\frac{\sum \sigma_g}{N} \geq \sqrt{\sigma_{\mathrm{LTS}}^2 + \sigma_T^2 + \sigma_c^2} + C\sigma_m \tag{6}$$

The set of markers is denoted as $A = \{A_1, A_2, A_3, \ldots, A_{N_{\mathrm{tag}}}\}$, where N_{tag} denotes the sum of markers and A denotes the set of markers. The uncertainty from the initial point to the boundary marker is summarized as $\sum \sigma_g$, where g denotes the index of the boundary marker.

N denotes the number of segments and can be obtained as follows:

$$N = \left\lceil \frac{\sum \sigma_g}{\sqrt{\sigma_{\mathrm{LTS}}^2 + \sigma_T^2 + \sigma_c^2} + C\sigma_m} \right\rceil \tag{7}$$

The reference Manhattan distance of each segment which denotes d_{Seg} can be calculated accordingly.

$$d_{\mathrm{Seg}} = \frac{d(T_{\mathrm{Start}}, A_g)}{N} \tag{8}$$

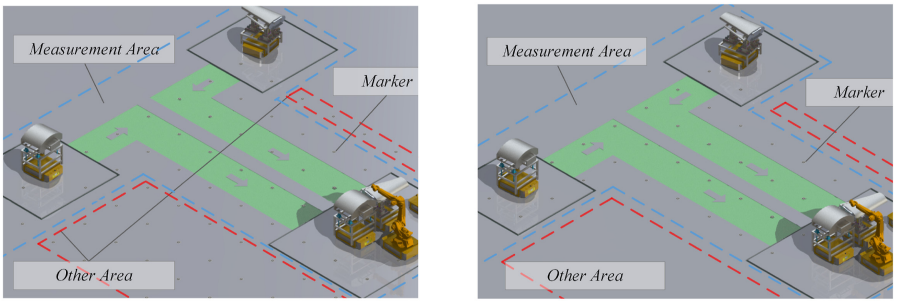

Markers in other area are not omitted **(a)**

Markers in other area are omitted **(b)**

Figure 4. The whole scene is divided into measurement area and other areas, as shown in (a) and (b) respectively

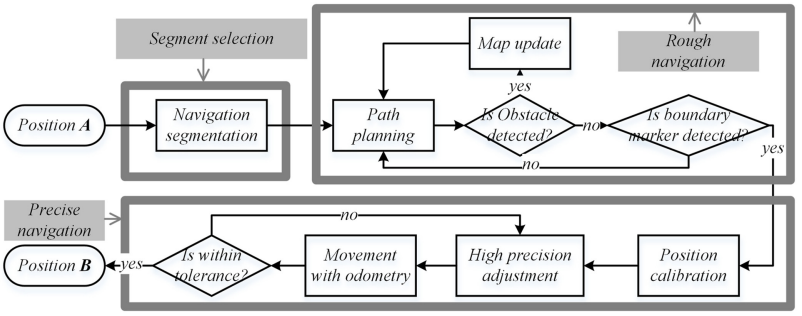

Figure 5. Process from position A to position B is segmented into segment selection, rough navigation and precise navigation

Interval of these markers closer to the reference distance and markers closer to the target station are selected as the segmented markers. The relationship of segmented markers can be expressed as follows:

$$i_j = \begin{cases} \left\| d(T_{\text{Start}}, A_{i_j}) - d(T_{\text{Start}}, A_{i_{j-1}}) - d_{\text{Seg}} \right\|_{\min} \\ d(T_{\text{Start}}, A_{i_j}) + d(A_{i_j}, T_{\text{Goal}}) = d(T_{\text{Start}}, T_{\text{Goal}}) \end{cases} \tag{9}$$

T_{Goal} denotes the position of the target station and $i_1, i_2, \ldots, i_N$ denotes the index of selected markers. Especially, $i_N = g$.

During the navigation, changes in direction (Censi *et al.*, 2013) will increase the count error of encoder and then reduce the accuracy of motion control. And routes with multiple turns are not allowed in the real measurement, because it will complicate the arrangement of measurement instruments.

$$g'(n) = \begin{cases} g(n-1) + k_{\text{same}}(g(n) - g(n-1)), D_{n-1,n} = D_{n-2,n-1} \\ g(n-1) + k_{\text{diff}}(g(n) - g(n-1)), D_{n-1,n} \neq D_{n-2,n-1} \end{cases} \tag{10}$$
$$f(n) = g'(n) + h(n)$$

To reduce the cost of changes in direction, the expansion direction of node denoted as $D_{n-1,n}$ is introduced. When the expansion direction of the node is the same as the previous one, the Manhattan distance of the expansion node is reduced to k_{same} times of the actual distance. When different, it will increase k_{diff} times.

The final positioning accuracy of AGV is more crucial for measurement. Generally, dynamic window approach (DWA) and virtual force field and other motion planning methods concentrate on the obstacle avoidance (Ryck *et al.*, 2020) rather than the final positioning. The positions of AGV are calibrated by boundary markers and then AGV with odometry (Kallasi *et al.*, 2017) is capable of high feedback accuracy at a short distance.

The DWA is optimized as follows.

$$G(v, w) = \alpha \cdot \text{angle}'(v, w) + \beta \cdot \text{dist}(v, w) + \gamma \cdot \text{vel}'(v, w) + \eta \cdot \text{dtar}(v, w) \tag{11}$$

In the above equation, taking into account the angle adjustment after the station, the angle evaluation function is optimized and adjusted.

$$\text{angle}'(v, w) = \begin{cases} 1 - \dfrac{\theta}{\pi}, \ \text{dtar}(v, w) > d_{M \text{ arg in}} \\ \dfrac{\theta - \theta_{\text{tar}}}{\pi}, \ \text{dtar}(v, w) \leq d_{M \text{ arg in}} \end{cases} \tag{12}$$

The remaining distance function is added to encourage the approaching. In the equation, d_{tar} is the distance between the current position and the goal, d_{tar0} is the distance between the calibrated position with markers and the goal and d_{sam} is the sampling distance (see Figure 6).

$$\text{dtar}(v, w) = \cos\left(\frac{d_{\text{tar}} + d_{\text{sam}}}{d_{\text{tar0}} + d_{\text{sam}}}\right) \tag{13}$$

The speed is reduced as the goal gets closer.

$$\text{vel}'(v, w) = \frac{v}{v_{\max}}, \ v \leq sin\left(\frac{d_{\text{tar}} + d_{\text{sam}}}{d_{\text{tar0}} + d_{\text{sam}}}\right) \bullet v_{\max} \tag{14}$$

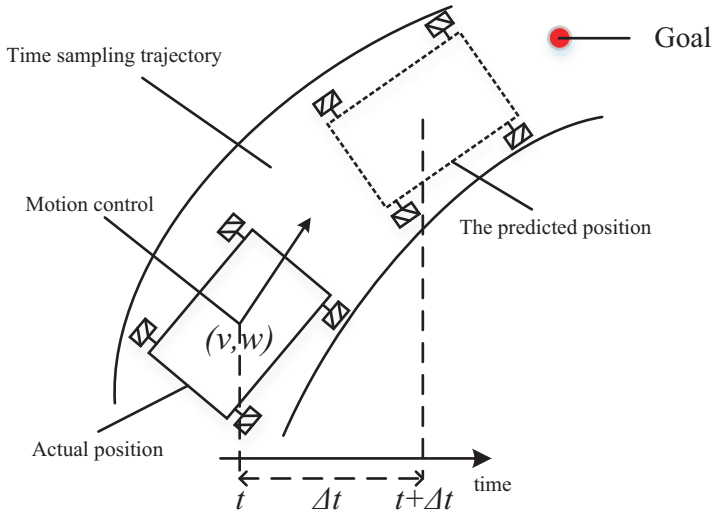

Figure 6.
Sampling space of DWA algorithm

5. Experiment

Markers are applied to improve the accuracy of the occupancy grid map, optimize the path planning method and calculate the adjustment with high accuracy, which plays a crucial role in the proposed navigation system. It is indispensable to verify the self-positioning accuracy of recognizing markers.

The laser tracker is a high-precision measuring device and it can be applied as ground truth for accuracy verification. And then, the accuracy of self-positioning can be verified with the markers. To verify the accuracy and efficiency of the proposed navigation method, several methods are experimented for comparison.

5.1 Accuracy of self-positioning

The process of the self-positioning is that AGV recognizes the marker and calculate the position of the AGV. The deviation of the visual self-positioning σ_{cam} has a vital effect on the positioning accuracy. In order to verify the reliability of the self-localization algorithm, the proposed marker based positioning method is compared with AMCL and NAV350 methods which are widely used in factory. As shown in Plate 3, the experimental equipment consists of AGV (repeatability: 0.1 mm), camera (type: MER2-503-36U3M/C-L, accuracy: 100l p/mm), markers (type: April Tag, size: 50 × 50 mm), LiDAR (type: Hokuyo UST-10LX, accuracy: ±40 mm), NAV350 laser scanner (accuracy: ±4 mm), laser tracker and the matching T-Probe (type: Leica AT901, accuracy: ±10 μm+5 μm/m).

The proposed positioning method is to achieve the positions of markers by the T-Probe and then to calculate the positions of AGV with cameras. The AMCL method is to build an occupancy grid map with SLAM and then to calculate the positions with AMCL algorithm. NAV350 obtains its precise position through the reflector. The positioning accuracy of different methods is compared with the reference, which is the position of AGV obtained by the laser tracker. Deviations will be negative when AGV has not reached the theoretical position, otherwise it will be positive. The three positioning methods are verified 20 times in each of the four markers and deviations with reference can be processed into the distributions of different directions as shown in Plate 3 and Table 1, where μ_{self} denotes the average

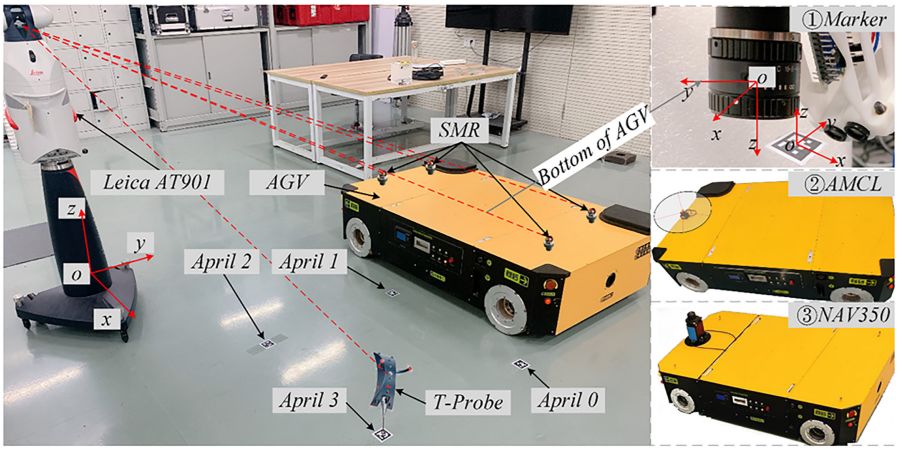

Plate 3.
Verification of self-positioning is carried out with marker, AMCL with LiDAR and NAV 350

Table 1.
The deviations of the positions acquired by self-positioning and the laser tracker

No	Marker based positioning method			AMCL positioning method			NAV350 positioning method		
	dx/mm	*dy*/mm	*dr*/mm	*dx*/mm	*dy*/mm	*dr*/mm	*dx*/mm	*dy*/mm	*dr*/mm
1	0.232	0.353	0.422	14.397	5.066	15.263	−0.042	0.011	0.043
2	0.298	0.342	0.453	0.552	−6.440	6.463	−0.139	−0.089	0.165
3	0.139	0.134	0.193	18.433	13.410	22.794	0.086	1.979	1.981
4	−0.360	0.194	0.409	31.407	17.210	35.813	0.444	0.951	1.050
5	−0.384	0.074	0.391	−0.416	13.670	13.676	−0.409	0.579	0.709
...	...	...	...	...	...	...	...	...	...
80	−0.249	−0.305	0.394	3.639	2.068	4.186	0.106	0.125	0.164
μ_{self}	−0.006	0.058	\	2.069	3.335	\	0.128	0.040	\
σ_{self}	0.282	0.254	\	12.923	11.836	\	0.989	1.068	\
$\pm 3\sigma_{self}$	0.846	0.762	1.139	38.769	35.508	52.572	2.967	3.204	4.367

deviation and σ_{self} denotes the standard deviation. *dr* represents the magnitude of the deviation, which does not follow the normal due to the loss of direction.

Figure 7 shows the deviations of three methods in direction *x* and *y*. The average positioning accuracy of the AMCL based algorithm is about ±52.572 mm, the accuracy of which is too large for the measurement. The average positioning accuracy of the proposed marker based method at four markers is ±1.139 mm and the widely used expensive Sick NAV350 is about ±4.367 mm, which shows that the proposed marker based methods is superior in positioning. Main reason for the difference in positioning is the difference of the reference. The references of three methods are markers, laser cloud points and reflectors. Combined with reflectors, NAV 350 uses the TOF (time of flight) method to directly measure the distance, which is more reliable than point clouds. The feature of markers is more obvious and easier than reflectors to be calibrated, so the positioning accuracy is highest among the three. In general, the proposed marker-based positioning method is more suitable for the cooperative measurement.

5.2 Accuracy and efficiency of navigation methods

The proposed navigation system makes full use of markers for cooperative measurement. As shown in Plate 4, the verification prototype consists of AGV, LiDAR (type: Hokuyo UST-

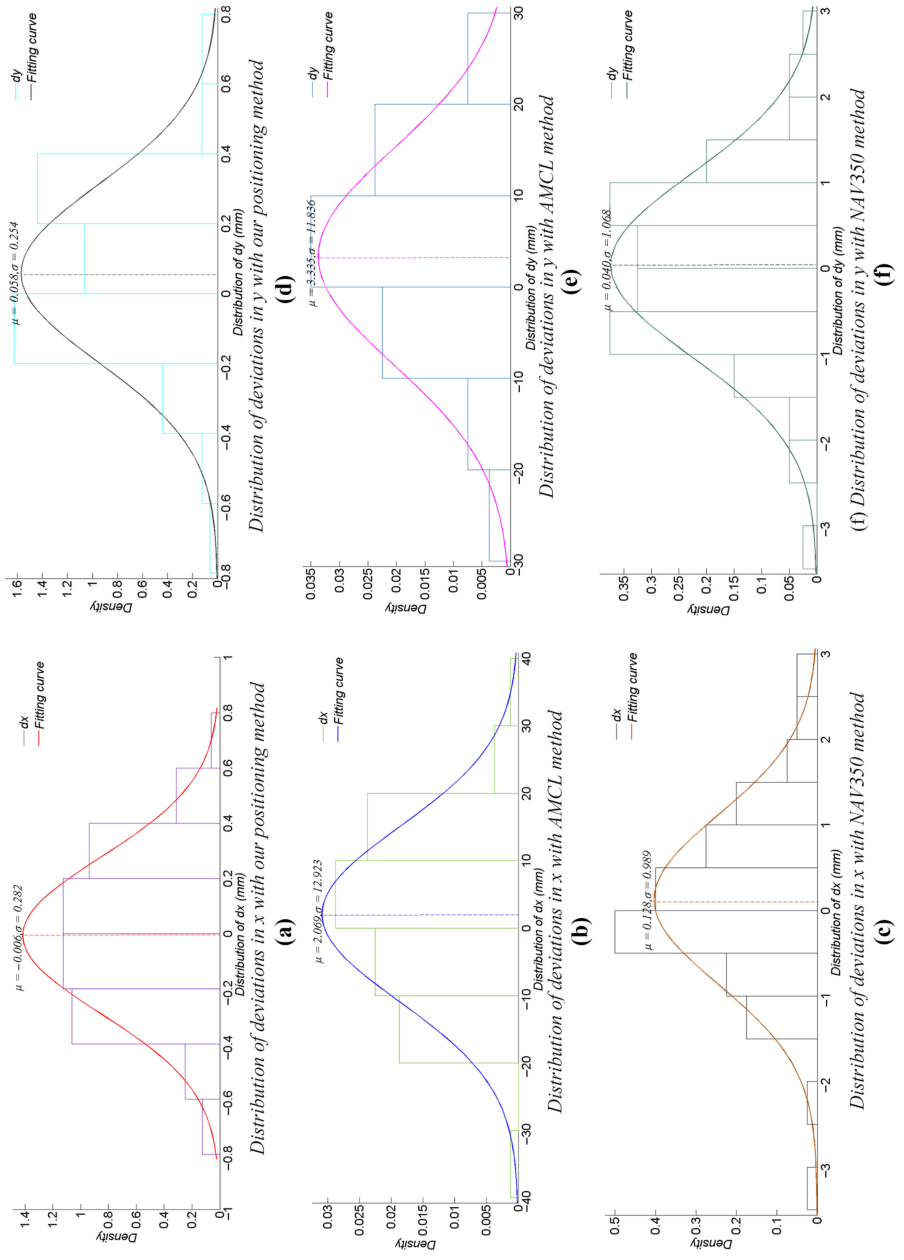

Figure 7.
Distributions of deviations in x and y are compared with three different methods

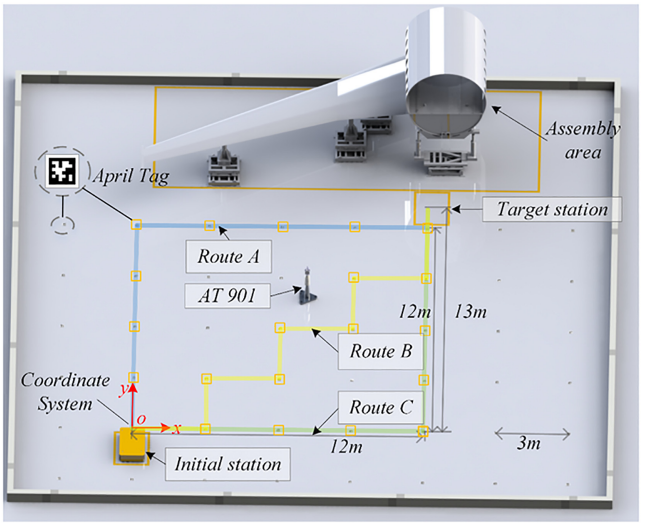

Plate 4.
Experimental verification prototype is constructed in the laboratory and the experiments are conducted

10LX, accuracy: ±4 mm), camera, laser tracker, April Tags at different intervals and three different routes and the experiment is carried out on the three routes. As shown in Figure 8, the cost of Route A is the least which is preferred by our path planning method and Route C is secondly preferred. Route B with multiple turns is selected to compare with Route A and Route C for the importance of reducing changes in direction. The proposed segmented navigation method is compared with the uniform distribution method utilized by Wang and the method without segmentation (Wang *et al.*, 2021).

The proposed method and Wang both segment the navigation into several segments. The difference is that the segmentation by Wang is based on multiple markers with same intervals and the interval is selected by estimation and experience. The proposed method selects the boundary marker first, and then calculates the specific navigation interval with proposed equations in advance. In order to fully compare with the uniform distribution

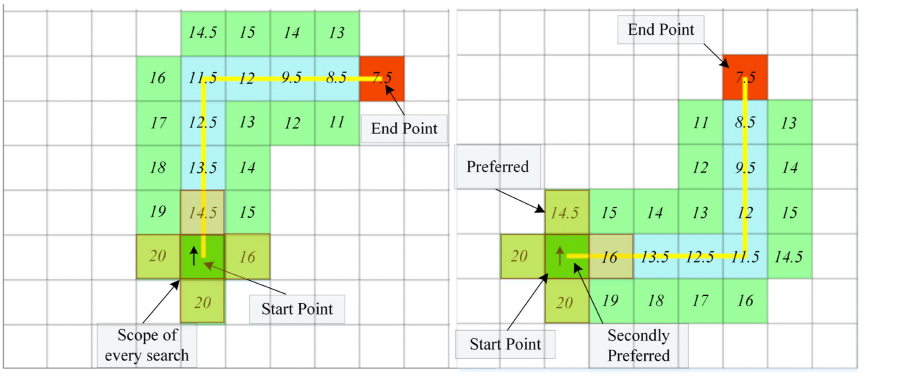

Preferred search with proposed method **(a)**

Secondly preferred search with the proposed method **(b)**

Figure 8.
The cost of Route A and Route C in path planning is shown and the difference is the cost chosen in the first search

method, several intervals of segmentations are designed. When the interval is five markers, AGV cannot guarantee recognizing the segment marker because of the accumulated deviation. To simplify the description, the different segmentation methods are denoted as several cases. Case I is that AGV moves without the help of markers. Case II, case III, case IV and case V are the uniform distribution from every one marker to every four markers, respectively. Case VI is the segmentation with the proposed method. At each route of the three paths, the three different navigation methods are all conducted and the average measurement results are shown in Figure 9 and Table 2. In Figure 9, the colorful grids represent the position of the measurement, and the color denotes the deviation. The distribution of deviations is shown in Table 2 where μ_p denotes the mean deviation, σ_p denotes the standard deviation and t denotes the cost time of navigation.

The average positioning accuracy and cost time of three routes are 7.6 mm, 8.4 mm, 8.0 mm and 150 s, 172.8 s, 154.8 s, respectively. The result shows that the cost time of Route A

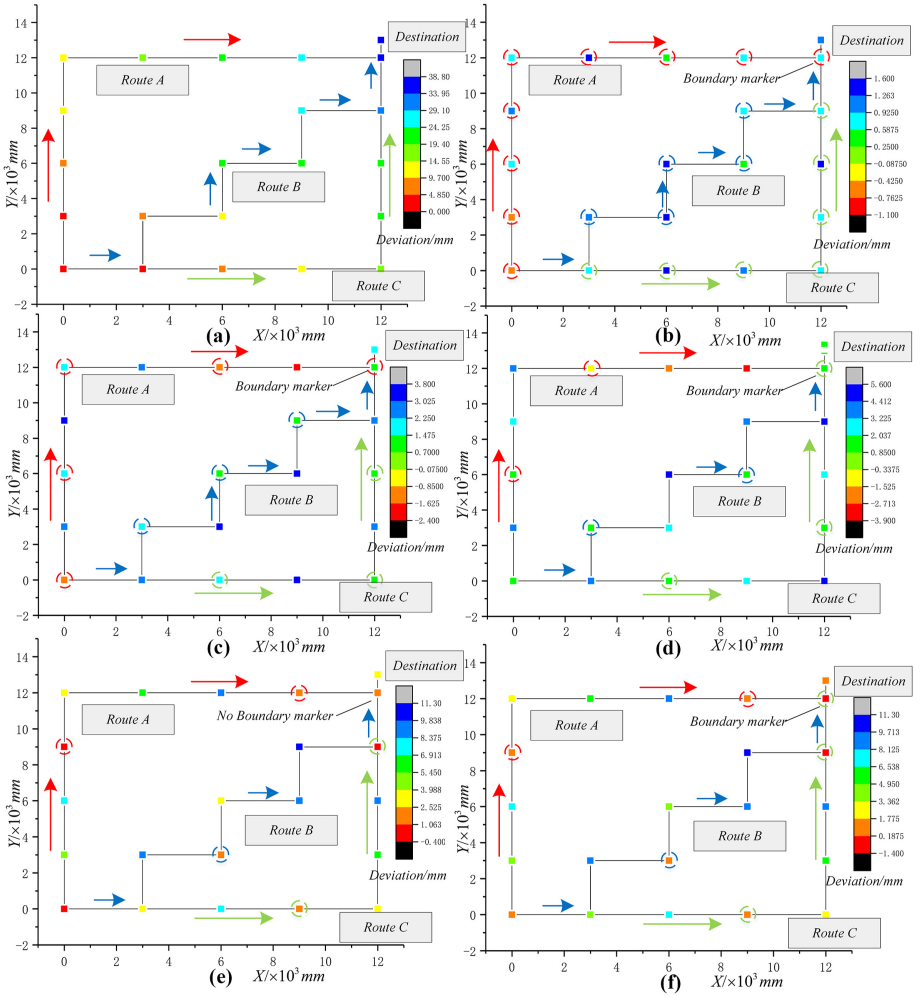

Figure 9.
Deviations with different segmentation methods: (a) to (f) are experiments from I to VI

Table 2.
Average deviation distribution of different navigation methods

Case	I			II			III			IV			V			VI		
Route	A	B	C	A	B	C	A	B	C	A	B	C	A	B	C	A	B	C
σ (mm)	33.3	37.9	36.8	1.6	2.1	1.7	2.1	2.4	2.0	1.9	1.8	2.1	5.1	4.1	3.8	1.8	2.1	1.7
μ_p (mm)	16.8	20.3	18.5	1.5	2.2	1.8	1.0	2.3	1.7	1.0	2.7	2.5	4.1	4.7	3.8	3.1	4.4	3.2
σ_p (mm)	11.2	13.1	12.4	1.1	1.5	1.3	1.6	2.1	1.2	1.6	1.7	1.5	2.5	3.6	3.0	2.7	3.8	3.4
t (s)	133	158	139	173	188	179	161	182	166	150	176	155	140	165	143	143	168	147

is 4.8 s less on average than on Route C, while the average positioning accuracy is 5.3% higher than that of Route C. The main reason for the difference is the steering of AGV at the first marker. Comparing with Route A, Route B with more turnings takes 15.2% more time and the accuracy of Route B is also 0.8 mm lower, which can prove that changes in direction do have an influence on the deviations and cost time.

The result of six cases is compared for the verification of segmentation methods. The cost time of case I is 13.3% shorter than other cases on average, while the positioning accuracy drops by 32.6 mm on average. The comparison shows that although the segmented navigation methods with markers cause a decrease in efficiency, it will significantly improve the positioning accuracy. The average positioning accuracy and cost time of cases with uniform distribution method are 1.8 mm, 2.2 mm, 1.9 mm, 4.3 mm and 180 s, 169.7 s, 160.3 s, 149.3 s, respectively. In general, the smaller the interval, the higher the positioning accuracy and the more time it takes. However, the comparison of case II, case III and case IV shows that the positioning accuracy is optimized no more than 4% while the cost time is increased by 12.3%. The variance becomes smaller, but the positioning accuracy has not improved significantly as the interval shrinks. The reason can be derived from the comparison with case V and case VI. Segmentation of case V and case VI is similar except the difference of the boundary marker. Case VI takes 2.3% more time while the final positioning accuracy increases by 48.8%. Boundary marker is the marker closest to the target station and it can reduce the cumulative error of odometry effectively. The boundary marker is all covered by case II, case III and case IV, so the positioning accuracy is not much different. Comparing with case II and case VI, the positioning accuracy is almost the same and enough for the measurement requirements of ± 5 mm, but the efficiency has increased by more than 17%. Synthetically, the proposed navigation method is relatively superior in the comparison and well applied for the cooperative measurement with high accuracy and efficiency.

6. Conclusions

This paper proposes a marker based high-precision LiDAR navigation system for cooperative measurement. The coupling method is improved by designing a coupling method and the interval of markers is calculated based on the uncertainty analysis. The proposed navigation method optimizes the path planning method with segmentation and improved A^*. The precise adjustment is completed with odometry near the boundary marker. The accuracy of self-positioning is verified with different positioning methods. The proposed navigation method is verified with several methods in our experimental prototype. In general, the proposed navigation system is efficient and flexible for the accurate aircraft cooperative measurement.

Future work will focus on the following areas:

(1) Applying the marker-based algorithms to the field of VSLAM;

(2) Adaptively improving the system for more aircraft assembly needs.

References

Andrea, R.D. (2012), "A revolution in the warehouse: a retrospective on kiva systems and the grand challenges ahead", *Automation Science and Engineering*, Vol. 9 No. 4, pp. 638-639.

Andreasson, H. (2015), "Autonomous transport vehicles: where we are and what is missing", *Robotics and Automation Magazine IEEE*, Vol. 22 No. 1, pp. 64-75.

Arun, K.S. (1987), "Least-squares fitting of two 3-D point sets", *IEEE Transactions on Pattern Analysis and Machine Intelligence*, Vol. 9 No. 5, pp. 698-700.

Censi, A., Franchi, A., Marchionni, L. and Oriolo, G. (2013), "Simultaneous calibration of odometry and sensor parameters for mobile robots", *IEEE Transactions on Robotics*, Vol. 29 No. 2, pp. 475-492.

Coope, I.D. (1993), "Circle fitting by linear and nonlinear least squares", *Journal of Optimization Theory and Applications*, Vol. 76 No. 2, pp. 381-388.

Deng, Z., Li, S. and Huang, X. (2018), "A flexible and cost-effective compensation method for leveling using large-scale coordinate measuring machines and its application in aircraft digital assembly", *Measurement Science and Technology*, Vol. 29 No. 6, 065904, p. 15.

Fiala, M. (2015), "ARTag, a fiducial marker system using digital techniques", *IEEE Computer Society Conference on Computer Vision and Pattern Recognition*, Vol. 2, pp. 590-596.

Flynn, R. and Miller, C. (2019), "11 Reasons to use automated metrology", SAE Technical Paper 2019-01-1369. doi: 10.4271/2019-01-1369.

Gao, X., Wang, J. and Chen, W. (2016), "Land-mark placement for reliable localization of automatic guided vehicle in warehouse environment", *IEEE International Conference on Robotics and Biomimetics IEEE*.

Garrido-Jurado, S. (2014), "Automatic generation and detection of highly reliable fiducial markers under occlusion", *Pattern Recognition*, Vol. 47 No. 6, pp. 2280-2292.

Hess, W., Kohler, D., Rapp, H. and Andor, D. (2016), "Real-time loop closure in 2D LIDAR SLAM", *IEEE International Conference on Robotics and Automation*, pp. 1271-1278.

Kallasi, F., Rizzini, D.L., Oleari, F., Magnani, M. and Caselli, S. (2017), "A novel calibration method for industrial AGVs", *Robotics and Autonomous Systems*, Vol. 94, pp. 75-88.

Krogius, M., Haggenmiller, A. and Olson, E. (2019), "Flexible layouts for fiducial Tags", *IEEE/RSJ International Conference on Intelligent Robots and Systems*, pp. 1898-1903.

Kudriashov, A., Buratowski, T. and Giergiel, M. (2019), "Hybrid AMCL-EKF filtering for SLAM-based pose estimation in rough terrain", *Mechanisms and Machine Science*, Vol. 73, pp. 2819-2828.

Liu, H., Zhu, W. and Ke, Y. (2017), "Pose alignment of aircraft structures with distance sensors and CCD cameras", *Robotics and Computer Integrated Manufacturing*, Vol. 48, pp. 30-38.

Mei, Z. and Maropoulos, P.G. (2014), "Review of the application of flexible, measurement-assisted assembly technology in aircraft manufacturing", *Proceedings of the Institution of Mechanical Engineers Part B Journal of Engineering Manufacture*, Vol. 228 No. 10, pp. 1185-1197.

Motai, Y. and Kosaka, A. (2008), "Hand-eye calibration applied to viewpoint selection for robotic vision", *IEEE Transactions on Industrial Electronics*, Vol. 55 No. 10, pp. 3731-3741.

Mur-Artal, R., Montiel, J.M.M. and Tados, J.D. (2015), "Orb-slam: a versatile and accurate monocular slam system", *IEEE Transactions on Robotics*, Vol. 31 No. 5, pp. 1147-1163.

Mur-Artal, R. and Tardos, J.D. (2017), "Orb-slam2: an open-source slam system for monocular, stereo and rgb-d cameras", *IEEE Transactions on Robotics*, Vol. 33 No. 5, pp. 1255-1262.

Olson, E. (2011), "AprilTag: a robust and flexible visual fiducial system", *IEEE International Conference on Robotics and Automation*, pp. 3400-3407.

Qin, Z., Peng, W., Jia, S., Lu, J. and Hong, Q. (2016), "Precise robotic assembly for large-scale objects based on automatic guidance and alignment", *IEEE Transactions on Instrumentation and Measurement*, Vol. 65 No. 6, pp. 1398-1411.

Ramasamy, S., Sabatini, R., Gardi, A. and Liu, J. (2016), "LIDAR obstacle warning and avoidance system for unmanned aerial vehicle sense-and-avoid", *Aerospace Science and Technology*, Vol. 55, pp. 344-358.

Röwekämper, J., Sprunk, C., Tipaldi, G.D., Stachniss, C. and Burgard, W. (2012), "On the position accuracy of mobile robot localization based on particle filters combined with scan matching", *IEEE/RSJ International Conference on Intelligent Robots and Systems*, pp. 3158-3164, doi: 10.1109/IROS.2012.6385988.

Ryck, M.D., Versteyhe, M. and Debrouwere, F. (2020), "Automated guided vehicle systems, state-of-the-art control algorithms and techniques", *Journal of Manufacturing Systems*, Vol. 54, pp. 152-173.

Vasiljevic, G., Miklic, D., Draganjac, I. and Kovacic, Z. (2016), "High-accuracy vehicle localization for autonomous warehousing", *Robotics and Computer Integrated Manufacturing*, Vol. 42, pp. 1-16.

Wang, J. and Olson, E. (2016), "AprilTag 2: efficient and robust fiducial detection", *IEEE/RSJ International Conference on Intelligent Robots and Systems*, pp. 4193-4198.

Wang, J., Tao, B., Gong, Z., Yu, S. and Yin, Z. (2021), "A mobile robotic measurement system for large-scale complex components based on optical scanning and visual tracking", *Robotics and Computer-Integrated Manufacturing*, Vol. 67, p. 67, doi: 10.1016/j.rcim.2020.102010.

Wu, D. and Du, F. (2018), "A parallel ranging-based relative position and orientation measurement method for large-volume components", *Journal of Sensors*, Vol. 3, pp. 1-11.

Xing, B., Zhu, Q., Pan, F. and Feng, X. (2018), "Marker-based multi-sensor fusion indoor localization system for micro air vehicles", *Sensors*, Vol. 18 No. 6, pp. 1706-1725.

Zeng, P., Wu, F., Zhi, T., Xiao, L. and Zhu, S. (2019), "Research on automatic tool delivery for CNC workshop of aircraft equipment manufacturing", *Journal of Physics: Conference Series*, p. 1215, 012007, doi: 10.1088/1742-6596/1215/1/012007.

Zeng, Q., Li, S., Deng, Z. and Huang, X. (2020a), "An error similarity-based error-compensation method for measurement in the non-uniform temperature field", *Measurement Science and Technology*, Vol. 31 No. 8, 085008.

Zeng, Q., Huang, X., Li, S.G. and Deng, Z.P. (2020b), "High-efficiency posture pre-alignment method for large component assembly via iGPS and laser ranging", *IEEE Transactions on Instrumentation and Measurement*, Vol. 69 No. 8, pp. 5497-5510.

Corresponding author
Xiang Huang can be contacted at: xhuang@nuaa.edu.cn